

LeanKAN: A Parameter-Lean Kolmogorov-Arnold Network Layer with Improved Memory Efficiency and Convergence Behavior

Benjamin C. Koenig, Suyong Kim,* and Sili Deng*

*Department of Mechanical Engineering, Massachusetts Institute of Technology,
77 Massachusetts Ave, Cambridge, MA 02139, United States.*

(Dated: February 26, 2025)

The recently proposed Kolmogorov-Arnold network (KAN) is a promising alternative to multi-layer perceptrons (MLPs) for data-driven modeling. While original KAN layers were only capable of representing the addition operator, the recently-proposed MultKAN layer combines addition and multiplication subnodes in an effort to improve representation performance. Here, we find that MultKAN layers suffer from a few key drawbacks including limited applicability in output layers, bulky parameterizations with extraneous activations, and the inclusion of complex hyperparameters. To address these issues, we propose LeanKANs, a direct and modular replacement for MultKAN and traditional AddKAN layers. LeanKANs address these three drawbacks of MultKAN through general applicability as output layers, significantly reduced parameter counts for a given network structure, and a smaller set of hyperparameters. As a one-to-one layer replacement for standard AddKAN and MultKAN layers, LeanKAN is able to provide these benefits to traditional KAN learning problems as well as augmented KAN structures in which it serves as the backbone, such as KAN Ordinary Differential Equations (KAN-ODEs) or Deep Operator KANs (DeepOKAN). We demonstrate LeanKAN's simplicity and efficiency in a series of demonstrations carried out across both a standard KAN toy problem and a KAN-ODE dynamical system modeling problem, where we find that its sparser parameterization and compact structure serve to increase its expressivity and learning capability, leading it to outperform similar and even much larger MultKANs in various tasks.

I. INTRODUCTION

Kolmogorov-Arnold Networks (KANs) [1, 2] are an emerging tool for data-driven and physics-inspired modeling. Traditional multilayer perceptrons (MLPs) contain predefined activation functions and learnable weights and biases to learn function approximations. KANs, on the other hand, apply the Kolmogorov-Arnold Theorem [3, 4] to instead learn the activation functions themselves, through gridded sums of univariate basis functions. These unique univariate activations are learned across all inputs, are then combined via parameter-free summation at each output. In other words, MLPs learn weights and biases with fixed activation functions, while KANs learn activation functions with fixed weights and biases. See Fig. 1(A) for a visual representation. This characteristic of learnable activation functions in KANs has shown to provide increased interpretability thanks to their visualizable profiles, rapid convergence with small parameter sizes thanks to their improved neural scaling laws, and the potential for human-readable output via sparse symbolic regression [1, 2, 5]. Mirroring the development trajectory of MLP-based networks through various augmented frameworks, KANs have been applied in architectures such as physics informed KANs [6–8], convolutional KANs [9], Deep Operator KANs [10], and KAN Ordinary Differential Equations [5]. Such applications retain the key inductive biases and physical insights embedded in these specialized structures (as originally studied in the standard MLP variants), while enabling the various inference benefits inherent to KANs, such as increased interpretability and high-order neural convergence.

While these applications have shown significant promise, the original KAN formulation of Liu et al. [1] on which they were built contains a key limitation to expressivity. With learnable univariate activations combined at each output only via addition, it is straightforward to express complex sums of univariate functions on two inputs x and y , such as $e^{\sin(x^2+y^2)}$, through gridded univariate basis functions combined via addition. It is surprisingly challenging, however, to represent even trivial multiplication such as xy . A theoretical two-input, one-output KAN layer combines the inputs x and y via learnable activations $f_a(x)$ and $g_a(y)$, to construct an output of the form $f_a(x) + g_a(y)$. To represent xy , there does not exist a single-layer KAN solution due to the lack of multiplication expression across inputs. To get around this, a two-layer KAN was seen in [1] to converge to the roundabout $xy = ((x + y)^2 - (x^2 + y^2))/2$ using four activations in the first layer, which is needlessly bulky especially in light of the typically sparse and shallow exact function reconstructions presented in the remainder of that work. This naturally called for the follow-up

* Corresponding authors: suyong@mit.edu, silideng@mit.edu

work (KAN 2.0) of Liu et al. [2], where MultKAN was proposed. This augmented structure begins with a similar formulation to a standard KAN layer (henceforth referred to as AddKAN), but adds additional activation functions to enable an additional multiplication sublayer. This sublayer directly encodes the multiplication operator, allowing for simple and easily interpretable expression of trivial multiplication-based functions, like xy , up to more complex functions involving multiplication, like $\sin(x)y^2$, with a single layer only. More mathematical detail is provided in Sec. IIB, with a visualization in Fig. 1(B). In the same example where AddKAN learns the activation functions $f_a(x)$ and $g_a(y)$ for an output value $f_a(x) + g_a(y)$, a single MultKAN layer would additionally learn the activation functions $f_m(x)$ and $g_m(y)$ in parallel, combine them via $f_m(x) + g_m(y)$, and then inject the multiplication operator by computing the final output as $[f_a(x) + g_a(y)] \cdot [f_m(x) + g_m(y)]$, i.e. the product of the original AddKAN output node with a newly-added MultKAN output node. Here, we see that xy can be learned trivially in a single layer using $f_a(x) = x, g_a(y) = 0, f_m(x) = 0$, and $g_m(y) = y$. To summarize, where AddKAN requires two layers and six activation functions to learn a roundabout form of simple multiplication between two inputs, MultKAN does so with a single layer comprising four activations (two of which are trivially equal to zero). The improvements in expressivity and memory efficiency resulting from this formulation change are evident. Additionally, the substantial reduction in bulk and complexity offers notable advantages in symbolic regression and sparse representation, which are crucial for many KAN applications [1, 2, 5].

Despite the partial success of MultKAN, its specific construction bars it from general use in multidimensional outputs (i.e., $[x^3y, x + y, xy^2]$ rather than simply xy). Certain output nodes see the multiplication operator while others are restricted to the addition operator only, which we demonstrate in this work to be a significant training bottleneck. For example, the hyperparameters in a MultKAN network may dictate that only the second and third output values are learned using the multiplication operator, making the second and third indices of $[x^3y, x + y, xy^2]$ easily learnable in a single layer but the first index impossible to learn for the same reason that AddKAN cannot learn xy . This was not an issue in the original MultKAN manuscript [2] where investigation involved scalar outputs only, but constrains the applicability and interpretability of MultKAN in many real physical problems of KAN modeling interest with multidimensional outputs [5, 11]. In a similar vein, the MultKAN implementation adds two new hyperparameters, increasing the complexity of potential user tuning with this new framework. Finally, in terms of quantitative performance drawbacks, the architecture of a MultKAN dictates that for a given node and grid structure, additional activation functions are required beyond what is needed for AddKAN, degrading the memory efficiency of the MultKAN structure and potentially impacting its training speed and convergence behavior. In the example discussed above, for example, the two-input, one-output AddKAN learns only two activations, $f_a(x)$ and $g_a(y)$, while the two-input, one-output MultKAN learns $f_a(x), f_m(x), g_a(y), g_m(y)$. It is clear that the MultKAN performs better in this case thanks to the multiplication operator enabling it to learn xy , but it also “wastes” two activations to do so: $g_a(y) = 0, f_m(x) = 0$. In all KAN layer structures, the number of parameters scales proportionally with the number of activations (while the addition and multiplication of activations are parameter-free), so the MultKAN here would appear to have twice the number of parameters necessary in the obvious case of learning xy via $f_a(x) \cdot g_a(y)$, with f and g as identity functions.

In this work, we propose LeanKAN which substantially improves expressivity, memory efficiency, and training speeds of the network. This entirely reformulated multiplication structure for KAN layers allows us to eliminate one of two added hyperparameters, completely revert the increase in parameter size (returning to a size equal to that of the corresponding AddKAN), and provide general use in KANs with multidimensional outputs while retaining the multiplication operator. An example LeanKAN structure is shown in Fig. 1(C). LeanKAN eliminates the $f_m(x)$ and $g_m(y)$ activations, which we find here to be unnecessary for effective training, allowing for direct learning of $xy = f_a(x) \cdot g_a(y)$. As a replacement for individual KAN layers themselves, we expect that LeanKAN can be widely adapted in currently active fields of PDE discovery and surrogate modeling without restriction to specific models. Therefore, any performance benefits have potential impact not only for improved efficiency in standard KAN applications as a function approximator, but also in improved efficiency as the backbone of any number of these augmented KAN structures such as physics-informed KAN, DeepOKAN, and KAN-ODEs.

Accordingly, we compare LeanKAN against the original MultKAN in a series of tests within two case studies: one in a standard KAN learning application to demonstrate the specific structural benefits of LeanKAN, and the other in a KAN-ODE application to demonstrate how these benefits can scale to already-developed, augmented KAN structures. In all cases, we find that the reduced activation and parameter size of LeanKAN does not deteriorate training dynamics or converged performance. In fact, the more compact and parameter-lean LeanKAN networks achieve slightly stronger metrics across the board, thanks to their more efficient use of parameters and activations.

	Structure	Features	
(A) AddKAN (Ref. [1])		Expressivity	+
		# of activations (memory efficiency)	12 (4 → 3 layer)
		Hyperparameter complexity	Baseline (Network size, Basis function, Normalizer, ...)
(B) MultKAN (Ref. [2])		Expressivity	+, ×
		# of activations (memory efficiency)	20 (12 for addition, 8 for multiplication)
		Hyperparameter complexity	Baseline + 2 more (n^a, k)
(C) LeanKAN (Our work)		Expressivity	+, ×
		# of activations (memory efficiency)	12 (≪ 20 in MultKAN)
		Hyperparameter complexity	Baseline + only 1 (n^{mu})

FIG. 1. Visualization of the three KAN layers referenced in this work, all with four inputs and three outputs. (A) A standard AddKAN [1]. (B) A standard MultKAN [2] with second-order multiplication ($k = 2$), and one addition/identity output node ($n^a = 1$). (C) Currently proposed LeanKAN with two multiplication input nodes ($n^{mu} = 2$). Black nodes indicate inputs, while all others are labeled with addition, multiplication, or blank identity operators. Note that all KAN network parameters are defined at the activation functions only, and all connections and operators are parameter-free. Opacity of activations and connections is varied to imply the relative importance of different activations (as in [1]). Note that MultKAN requires 20 activations compared to AddKAN and LeanKAN’s 12 (with a proportional increase in parameters and memory), with even more required for larger n^a or k hyperparameters.

II. BACKGROUND

A. Traditional Kolmogorov-Arnold Network (AddKAN or KAN 1.0)

Standard MLP networks train fixed activation functions with learnable weights and biases, leveraging the universal approximation theorem [12] to accomplish learning tasks. KANs, on the other hand, rely on the Kolmogorov-Arnold representation theorem (KAT) [3] to train learnable activation functions. More specifically, the KAT states that any smooth and continuous multivariate function $f(\mathbf{x}) : [0, 1]^n \rightarrow \mathbb{R}$ can be represented as a finite sum of continuous univariate functions,

$$f(\mathbf{x}) = f(x_1, \dots, x_n) = \sum_{q=1}^{2n+1} \Phi_q \left(\sum_{p=1}^n \phi_{q,p}(x_p) \right). \quad (1)$$

Here, $\phi_{q,p} : [0, 1] \rightarrow \mathbb{R}$ are the univariate activation functions evaluated on the inputs x_p to construct the q^{th} node of the hidden layer, while $\Phi_q : \mathbb{R} \rightarrow \mathbb{R}$ are the second layer’s activation functions that construct the scalar output from the hidden layer node values (overall representing a two-layer KAN with a hidden layer width of $2n + 1$ and an output dimension of 1). In matrix form, the n_{l+1} -dimensional output of a single KAN layer with n_l inputs can be represented as

$$\mathbf{y} = \Phi_l \mathbf{x} \in \mathbb{R}^{n_{l+1}}, \quad (2)$$

TABLE I. Comparison of AddKAN, MultKAN, and LeanKAN.

	AddKAN	MultKAN	LeanKAN
Operators Encoded	Addition	Addition and Multiplication	Addition and Multiplication
Structural Limitation	None	Multidimensional output layers	Multidimensional input layers
Number of Activation Functions (\propto Number of Parameters)	$n_l \cdot n_{l+1}$	$n_l \cdot n_{l+1} + \underbrace{n_l(k-1)n^m}_{\text{increased}}$ [note $n^m = n^{l+1} - n^a$, $k \geq 2$.]	$n_l \cdot n_{l+1}$
Multiplication	N/A	n^a (# of additive nodes)	n^{mu} (# of multiplicative nodes
Hyperparameters		k (multiplication order)	and multiplication order)
Reference	Ref. [1]	Ref. [2]	This work

where Φ_l combines the trainable activation functions seen in Eq. 1, resulting in

$$\Phi_l = \begin{pmatrix} \phi_{l,1,1}(\cdot) & \phi_{l,1,2}(\cdot) & \cdots & \phi_{l,1,n_l}(\cdot) \\ \phi_{l,2,1}(\cdot) & \phi_{l,2,2}(\cdot) & \cdots & \phi_{l,2,n_l}(\cdot) \\ \vdots & \vdots & & \vdots \\ \phi_{l,n_{l+1},1}(\cdot) & \phi_{l,n_{l+1},2}(\cdot) & \cdots & \phi_{l,n_{l+1},n_l}(\cdot) \end{pmatrix}, \quad (3)$$

where ϕ is the activation function with subscripts l indicating the index of the current layer, n_l indicating the number of nodes in the current layer, and n_{l+1} indicating the number of nodes in the subsequent layer. In other words, each input is connected to each output with a unique learnable activation function, leading to a total of $n_l \cdot n_{l+1}$ activation functions connecting the l^{th} and $(l+1)^{\text{th}}$ layers. An AddKAN layer with four inputs and three outputs is shown in Fig. 1(A), with a corresponding 12 activation functions. Finally, by stacking this AddKAN layer (Eq. 2), a multi-layer KAN can be constructed such that $\text{KAN}(\mathbf{x}) = (\Phi_{L-1} \circ \Phi_{L-2} \circ \cdots \circ \Phi_1 \circ \Phi_0) \mathbf{x}$.

The original KAN implementation used B-splines as the basis functions that comprise each activation, although it was later shown in Li [13] that Gaussian radial basis functions (RBFs) are more efficient. Here, we define the individual activation functions as

$$\phi_{l,\alpha,\beta}(\mathbf{x}) = \sum_{i=1}^N w_{l,\alpha,\beta,i}^\psi \cdot \psi(\|\mathbf{x} - \mathbf{c}_i\|) + w_{l,\alpha,\beta}^b \cdot b(\mathbf{x}), \quad (4)$$

$$\psi(r) = \exp\left(-\frac{r^2}{2h^2}\right), \quad (5)$$

where N is the grid size (number of gridded basis functions used to reconstruct a single activation), $w_{l,\alpha,\beta,i}^\psi$ and $w_{l,\alpha,\beta}^b$ are the learnable parameters that scale and superimpose the RBF basis functions $\psi(r)$ and the base activation function $b(\mathbf{x})$, respectively, α and β are the index of the layer l 's matrix in Eq. 3 on which these weights are applied, \mathbf{c}_i are the centerpoints of each gridded basis function, and h is the gridpoint spacing (i.e. the RBF spreading parameter). Normalization is carried out at each layer as in Refs. [14, 15], to avoid the original and expensive re-gridding technique of Liu et al. [1]. Base activations $b(\mathbf{x})$ are directly defined as Swish activation functions [16].

B. Multiplication Kolmogorov-Arnold Network (MultKAN or KAN 2.0)

The subsequent work of the original KAN authors [1] introduced MultKAN [2], which augments the summation terms in Eq. 1 with optional multiplication connections, allowing for more inherent expressivity while training and when symbolically expressing functions. MultKAN starts from an identical construction as AddKAN, where an input \mathbf{x} is transformed via the activation function matrix Φ into \mathbf{y} (as in Eqs. 2 and 3), where \mathbf{y} is defined here as a hidden subnode output rather than the final layer output. Then, to compute the true layer output \mathbf{z} , an auxiliary

activation-free (and thus parameter-free) layer Ω_l is defined in Eq. 6 as per the following notation in Python for l^{th} layer.

$$\mathbf{z}_l = \Omega_l \mathbf{y}_l = \underbrace{[\mathbf{y}_l[1 : n_{l+1}^a]]}_{\text{identity}}, \underbrace{[\mathbf{y}_l[n_{l+1}^a :: 2] \odot \mathbf{y}_l[n_{l+1}^a + 1 :: 2]]}_{\text{MultKAN segment } (k=2)} \in \mathbb{R}^{n_{l+1}^a + n_{l+1}^m}. \quad (6)$$

Here, the sublayer \mathbf{y}_l with n_{l+1} output nodes is split into n_{l+1}^a addition-only nodes and $n_{l+1}^m = n_{l+1} - n_{l+1}^a$ multiplication nodes. The mapping from \mathbf{y} to \mathbf{z} performs no operations for the first n_{l+1}^a identity nodes of \mathbf{z} (“identity”). For the remaining n_{l+1}^m nodes of \mathbf{z} , however, k^{th} order multiplication is carried out on the subnode y values (“MultKAN segment”), where we define “order” in this case as the number of activations included in the product (i.e. $y_1 \cdot y_2$ is second order, $y_1 \cdot y_2 \cdot y_3$ is third order). Here the hyperparameter $k = 2$ leads to second order, pairwise multiplication as denoted by \odot , while higher values of k would encode higher-order multiplication terms in the MultKAN segment of this equation. A MultKAN layer with four inputs and three outputs is shown in Fig. 1(B), where $n_{l+1}^a=1$ dictates that $z_1 = y_1$ (“identity”), while z_2 and z_3 are the respective pairwise products of y_2 and y_3 ; and y_4 and y_5 (“MultKAN segment”). To facilitate pairwise multiplication for z_2 and z_3 with this set of hyperparameters, we see that two additional nodes in the \mathbf{y} layer are required. These added nodes increase the number of activations to 20, a 66% increase from the 12 needed in the same structure for AddKAN (see Fig. 1(A)). We note that in any case with $n_{l+1}^m \neq 0$, the dimension of $\mathbf{y} \in \mathbb{R}^{n_{l+1}^a + k n_{l+1}^m}$ is larger than the dimension of $\mathbf{z} \in \mathbb{R}^{n_{l+1}^a + n_{l+1}^m}$ by $(k-1)n_{l+1}^m$, in order to facilitate these multiplication connections. This leads to a proportional increase in activation functions (and identically in the number of parameters).

Due to the increased number of activations needed for multiplication, MultKAN exhibits inflation of the total number of parameters in a given layer, especially for higher-order multiplication (i.e. $k > 2$). In other words, MultKAN has a parameter count strictly larger than a standard AddKAN, even for an identical layer structure (input nodes, output nodes, and grid size). Therefore, while it benefits from the inclusion of the multiplication operator and any inherent representation capability or expressivity contained therein, the MultKAN structure is also hypothesized here to deteriorate memory efficiency and reduce training speeds as a result of this parameter inflation.

Another limitation of this MultKAN implementation is that it is not generally applicable in the last layer of a multi-output KAN. We see in Eq. 6 that the array of output nodes \mathbf{z}_l has certain indices (up to n_{l+1}^a) that include only identity transformations of the subnode inputs \mathbf{y}_l , while other indices ($n_{l+1}^a + 1$ to the end) include multiplicative transformations of the subnode inputs. This asymmetrical structure can lead to performance degradation with multidimensional output layers, where for example if an output vector includes $z_i = x_1 \cdot x_2$ where $i < n^a$, i.e. $z_i = y_i$ with no multiplication terms, then MultKAN has effectively reverted to AddKAN due to the lack of multiplication on the \mathbf{y} sublayer for the z_i output, making $x_1 \cdot x_2$ impossible to learn in a single layer.

Finally, we highlight that hyperparameter tuning is made more complex when switching from a standard KAN to a MultKAN, as two new hyperparameters are added: k , which dictates the multiplication order or number of activations that are multiplied together to arrive at each node, and n^a , which dictates how many of the nodes in each layer are additive vs. multiplicative.

III. METHOD

A. Parameter-Lean Kolmogorov-Arnold Network (LeanKAN)

We propose LeanKAN, an entirely reformulated KAN layer with addition and multiplication nodes that can resolve these three identified issues in MultKAN. Rather than a standard addition layer Φ with optional multiplication layers Ω stacked on top such that $\mathbf{z} = \Omega \mathbf{y} = (\Omega \circ \Phi) \mathbf{x}$ as in MultKAN, we instead incorporate the multiplication layers directly into the computation of the subnode \mathbf{y} , replacing certain addition connections with multiplication rather than stacking multiplication on top of them. More specifically, starting from an n_l -dimensional input \mathbf{x} to the layer l and with an output \mathbf{z} of dimension n_{l+1} , we apply the gridded basis functions of Eq. 3 to the input to create the traditional KAN activations as in AddKAN, where the gridding and parameterization are all contained in the $\phi_{l,i,j}$ functions that make up Φ_l (see Eqs. 4 and 5). However, in contrast to Eq. 2 where matrix multiplication immediately sums this $n_{l+1} \times n_l$ matrix of activations into the n_{l+1} -dimensional output vector, here we split the activation matrix into separate multiplication and addition components. Specifically, we define a single hyperparameter n^{mu} (to differentiate from n^m in MultKAN, Eq. 6) dictating the number of multiplication input nodes, with n^{add} defined implicitly via $n_l^{add} = n_l - n_l^{mu}$. Then, the hidden nodes can be expressed by

$$y_{l,i}^{\text{mult}} = \prod_{j=1}^{n_l^{\text{mu}}} \phi_{l,i,j}(x_{l,j}) \quad \text{for } i \in \{1, 2, \dots, n_{l+1}\} \subset \mathbb{N}, \quad (7)$$

$$y_{l,i}^{\text{add}} = \sum_{j=n_l^{\text{mu}}+1}^{n_l} \phi_{l,i,j}(x_{l,j}) \quad \text{for } i \in \{1, 2, \dots, n_{l+1}\} \subset \mathbb{N}. \quad (8)$$

In essence, this formulation splits the inputs into two groups based on the ratio of n^{mu} and n^{add} , then independently takes the product and sum within the two groups to eliminate the input dimension j of the activation matrix Φ_l and arrive at the output vector \mathbf{y} . We contrast this against MultKAN, where the input dimension j of Φ_l is eliminated via summation only, requiring additional terms in the sublayer dimension (recall MultKAN’s \mathbf{y} sublayer being of higher dimension than the real output \mathbf{z}) to facilitate pairwise multiplication. Finally, to arrive at the output \mathbf{z} , we simply sum \mathbf{y}^{mult} and \mathbf{y}^{add} in the l^{th} layer,

$$\mathbf{z}_l = \mathbf{y}_l^{\text{mult}} + \mathbf{y}_l^{\text{add}} \in \mathbb{R}^{n_{l+1}}. \quad (9)$$

As previously, n_{l+1} is the number of outputs, making $\mathbf{z}_l \in \mathbb{R}^{n_{l+1}}$. A LeanKAN layer with four inputs and three outputs is shown in Fig. 1(C), with the sublayer labeled with \mathbf{y}^{mult} and \mathbf{y}^{add} demonstrating an equal split between addition and multiplication subnode operations ($n^{\text{mu}} = n^{\text{add}}$). To summarize, a MultKAN layer includes a standard AddKAN sublayer stacked with an optional multiplication sublayer. LeanKAN, on the other hand, directly modifies the AddKAN sublayer itself to split the nodes between addition and multiplication.

B. Structural Benefits of LeanKAN

This new layer design can be used in the output layer without loss of expressivity. By applying the addition sublayer in Eq. 9 after the combined multiplication sublayer (rather than before, as in MultKAN), we allow all output nodes to experience the effects of both multiplication and addition, regardless of the specific n^{mu} used.

Additionally, while MultKAN inflates the number of parameters included in each multiplication node (relative to a standard addition node) linearly with k in order to perform k^{th} order multiplication, in LeanKAN we do not perform any augmentation of subnode sizes and directly use the order of multiplication equal to n^{mu} . In doing so, we achieve a parameter count for a given node structure (e.g., four inputs and three outputs) that is exactly equal to the parameter count used in a traditional AddKAN, and is strictly smaller than that used in a MultKAN, even with the smallest $k = 2$ MultKAN value. See this comparison made explicitly in Fig. 1.

This modification not only preserves a parameter-lean structure, but also eliminates the k hyperparameter, instead rolling it into the single n^{mu} hyperparameter, where the multiplication order is specified directly by the number of input nodes selected for multiplication. We find that this does not penalize the performance of LeanKAN (and in fact appears to enhance its performance), while simplifying the hyperparameter tuning process by eliminating a degree of freedom. Table I summarizes these key differences between MultKAN and LeanKAN.

Finally, we emphasize that unlike most KAN augmentation architectures which implement additional treatments around standard KAN layers such as operator learning [10], physics enforcement [6–8, 17], or ODE coupling [5], the current methodology is developed as a direct and modular replacement for the standard KAN layers themselves, and can generally be applied to any of these augmented KAN structures as originally done with AddKAN and MultKAN layers. In the section of Experiments and Results, we demonstrate the key benefits of LeanKAN identified here in greater detail. All implementation used in the current work starts from the standard AddKAN repository of [15], with modifications carried out to implement MultKAN and LeanKAN.

IV. EXPERIMENTS AND RESULTS

A. LeanKAN as a Multidimensional Function Approximator

In this experiment, we compare the capabilities of MultKAN and LeanKAN when given multidimensional inputs and outputs, and discuss how the streamlined structure of LeanKAN lends it to significantly increased memory efficiency, with sparser parameterizations that can improve training dynamics and interpretability. We design the problem with

four input nodes $\mathbf{x} = [x_1, x_2, x_3, x_4]^\top$ and four output nodes $\mathbf{z} = [x_1x_2, x_3x_4, x_1x_2, x_3x_4]^\top$. In other words, we try to train KAN approximators for the following model:

$$\mathbf{z} = f([x_1, x_2, x_3, x_4]^\top) = [x_1x_2, x_3x_4, x_1x_2, x_3x_4]^\top, \quad (10)$$

where f is the target function to be learned. Here, we construct both MultKAN and LeanKAN with a single layer and a four-point grid using radial basis functions ψ for each activation function ϕ . The hyperbolic tangent normalization function and swish residual activation functions are implemented [16]. Values for $[x_1, x_2, x_3, x_4]^\top$ are uniformly generated between 0 and 1, with 150 training samples and 50 testing samples selected randomly (and identically across the MultKAN and LeanKAN sample sets). The same ADAM [18] learning rate of $1 \cdot 10^{-3}$ is used for both architectures.

1. Structural Biases of MultKAN and LeanKAN

The seemingly redundant \mathbf{z} values demonstrate how the two distinct network structures of MultKAN and LeanKAN compose their output values differently. In MultKAN (Fig. 2(A)),

$$z_1 = y_1 = \sum_{i=1}^4 \phi_{1,i}(x_i), \quad (11)$$

$$z_2 = y_2 = \sum_{i=1}^4 \phi_{2,i}(x_i), \quad (12)$$

$$z_3 = y_3 \cdot y_4 = \left(\sum_{i=1}^4 \phi_{3,i}(x_i) \right) \left(\sum_{i=1}^4 \phi_{4,i}(x_i) \right), \quad (13)$$

$$z_4 = y_5 \cdot y_6 = \left(\sum_{i=1}^4 \phi_{5,i}(x_i) \right) \left(\sum_{i=1}^4 \phi_{6,i}(x_i) \right). \quad (14)$$

Eqs. 11–14 show that z_1 and z_2 are composed of the addition of univariate functions, while z_3 and z_4 take products of two groups of sums (as per $k = 2$). Therefore, each node in the output layer possesses different levels of expressivity, and performs different operations on the subnode inputs. While z_3 and z_4 can easily reconstruct x_1x_2 and x_3x_4 respectively thanks to the multiplication of activations in Eqs. 13 and 14, z_1 and z_2 are effectively treated as AddKAN output nodes with summations only in Eqs. 11 and 12, and thus are not capable of expressing x_1x_2 or x_3x_4 . In contrast, LeanKAN (Fig. 2(B)) is designed to have an equal level of expressivity with multiplication and addition for all nodes in the output layer such that

$$z_k = y_k + y_{k+4} = \phi_{1,k}(x_1) \phi_{2,k}(x_2) + \phi_{3,k}(x_3) + \phi_{4,k}(x_4), \quad (15)$$

for all $k \in \{1, 2, 3, 4\}$, such that each output performs identical operations on its corresponding set of subnode inputs. Thus, all the nodes in the output layer are equally capable of learning multiplicative operations as well as additive operations. A limitation of this reformulation is that the LeanKAN layer studied here constrains multiplications to be on x_1 and x_2 only, with addition only on the remaining x_3 and x_4 . Therefore, the expression limits are shifted from output in MultKAN (Eq. 11–14) to input in LeanKAN (Eq. 15), making only z_1 and z_3 learnable with LeanKAN. This tradeoff can be seen visually in the network depictions of Fig. 2(A) and (B), where the nodes that “see” the multiplication operator are highlighted in both layer structures, as well as in the training profiles of Fig. 2(C) and (D), where it is seen that only the multiplication-seeing nodes are able to train properly. In practice, the corresponding limitations of these two networks can be overcome by using multi-layer structures, where the fully-connected nature of each independent layer distributes the multiplication operator across all inputs and outputs. Regardless, we find it important to report these limitations in light of the prevalence of single-layer KAN structures in the literature [1, 2, 5].

2. Improved Memory Efficiency for Training Performance and Interpretability

In addition to a tradeoff in single-layer expressivity, the newly proposed LeanKAN exhibits significant further benefits (without corresponding limitations) in terms of memory efficiency, accuracy, practitioner-friendly output layer

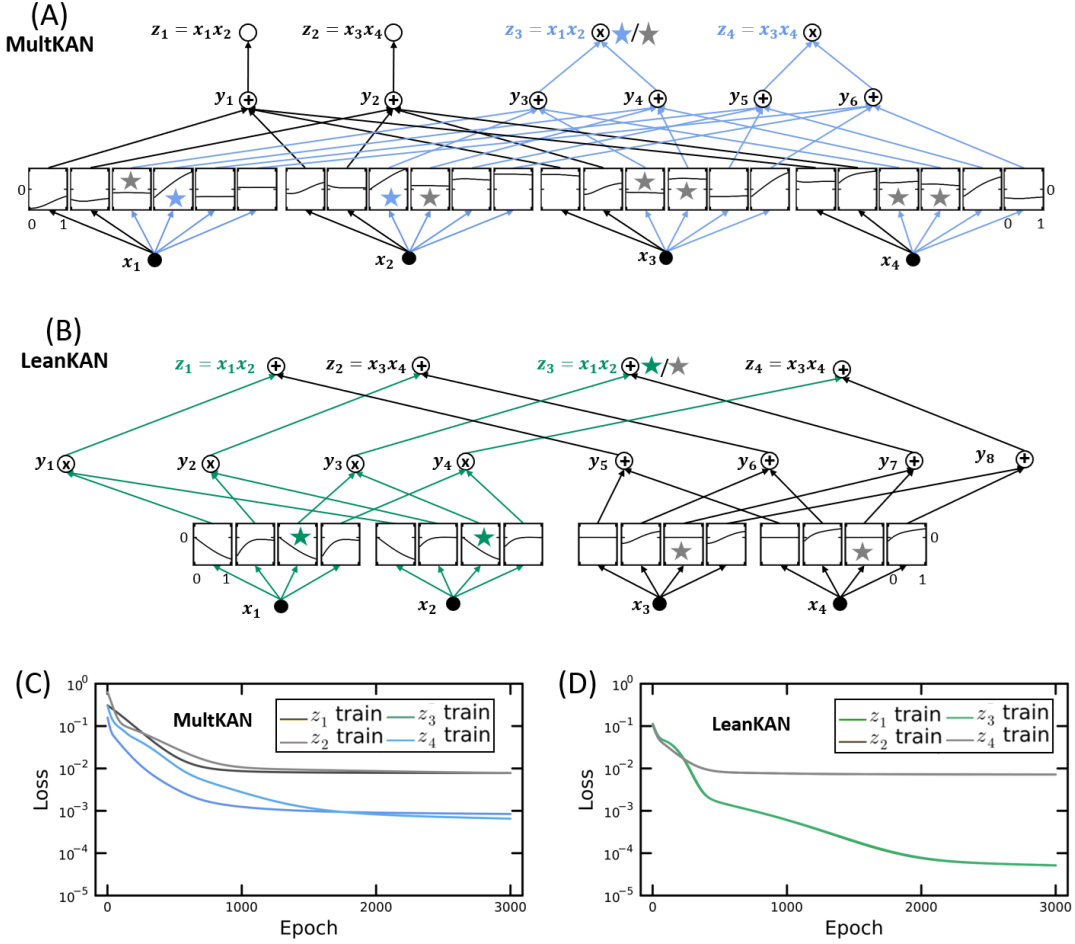


FIG. 2. Comparison between MultKAN and LeanKAN for single-layer multiplication training example. (A-B) Minimal MultKAN and LeanKAN structures that enable the second order multiplication required in this example ($k = 2$ and $n^a = 2$, or $n^{mu} = 2$, respectively). Connections and output node labels with access to the multiplication operator are highlighted in blue or green for MultKAN and LeanKAN, respectively. All activations connected to z_3 are labeled with either a colored (blue for MultKAN, green for LeanKAN) or grey star for nodes encoding the actual output behavior and dummy nodes, respectively. (C-D) Training dynamics for the same two respective networks, given 3,000 epochs. Note that the legends change between subfigures, corresponding to the change in learnable outputs in (A-B). Strongly overlapping dynamics in (D) lead to only two visible traces.

interpretation, and hyperparameter count. As reported in Table I, memory efficiency is substantially improved with LeanKAN. In a standard AddKAN layer with four inputs and four outputs, each input generates four parameterized activations, which sum into the respective outputs. In MultKAN, as seen in Fig. 2(A), this is increased to six activations per input, as $k = 2$ dictates that double the activations are required for the $4 - n^a = 2$ multiplication nodes. This change can also be seen in Eqs. 13 and 14, which have double the total activations on the right hand side. These additional activations increase the number of total parameters by 50%, from 80 to 120. Notably, this is the most parameter-efficient k hyperparameter possible with MultKAN, with higher values of k linearly increasing this scaling through additional sum terms in the products of Eqs. 13 and 14. In contrast, LeanKAN retains the exact number of activations (and thus parameters) as the corresponding AddKAN: four per input, with 80 total parameters.

The increased parameter count in MultKAN does not add nodes, layers, or other structures that might directly aid in the inference procedure and improve its performance relative to LeanKAN. It instead appears to be spent generating a substantial number of dummy (or non-meaningful) activation function terms. For instance, to express $z_3 = x_1 x_2$, MultKAN has eight activation functions ϕ in Eq. 13 but a majority of them (six out of eight) are not necessary to learn $x_1 x_2$. On the contrary, the LeanKAN architecture only needs four activation functions, half of which contribute to the expression of $x_1 x_2$. Without an explicit need for these bulky distributed multiplication terms (e.g., prior physical knowledge of some unique system), we find their inclusion intuitively unnecessary, especially in the physics modeling applications originally proposed in [2] that typically involve relatively compact functional

forms more closely resembling LeanKAN’s sparse Eq. 15 than the sixteen-term products of MultKAN’s Eq. 13-14. Quantitatively, we support this claim by highlighting that even with this reduced number of activation functions and reduced number of parameters, LeanKAN is remarkably able to improve on the performance of MultKAN by over an order of magnitude across all useful metrics (i.e. training and testing losses for the two properly-learned outputs), as seen in Fig. 3 (and identically in Figs. 2(C-D)). Contextualized in the 33% reduction in parameters (80 in LeanKAN vs 120 in MultKAN), this performance improvement is fairly remarkable, and suggests promise for the LeanKAN structure.

The current toy case additionally allows for close inspection of the activation function shapes to provide another angle on this analysis. In Fig. 2(A), the eight MultKAN activations used to reconstruct z_3 are labeled with a blue or grey star for the meaningful activations and the extraneous “dummy” activations, respectively. The same is done with green and grey stars for the four LeanKAN activations reconstructing z_3 in Fig. 2(B). In the LeanKAN, the two extraneous activations are effectively zeroed out, leaving the two meaningful activations with clean representations of $-x_1$ and $-x_2$, which are then multiplied together to arrive neatly at $z_3 = x_1x_2$. In contrast, MultKAN’s extraneous activations appear to have found local minima at fixed offsets that have to balance each other out in order to reconstruct z_3 . Specifically, the third activation of x_2 is, similarly to LeanKAN, a clean identity function. However, this is summed at y_3 with the third activations of x_1 , x_3 , and x_4 , which unlike in the LeanKAN now have roughly constant offset values that cancel each other out at the y_3 addition node. Similarly, the fourth activation of x_1 encodes the useful linear function needed here, but it has a negative offset. To counteract this, the fourth dummy activations of the remaining inputs similarly learn fixed offset values, although this time summing to a slightly positive value to correct the fourth activation of x_1 . The end result here is twofold. Mathematically, LeanKAN is able to rapidly converge its meaningful nodes to the correct behavior, as the dummy nodes are sparse and easily zeroed out; while MultKAN appears to converge more slowly, as the dummy nodes introduce local minima and non-optimal behavior via their bulkier sums and products that hinder the learning of the true underlying model. In terms of qualitative interpretability, LeanKAN’s lean architecture enables more direct interpretation of the activation functions ($z_3 = x_1x_2$), while MultKAN’s various offsets and constant activations conceal the true underlying function. While both structures would likely converge well to the trivial output studied here if given enough epochs, LeanKAN is able to do so much faster, with fewer parameters, and in a more interpretable way.

While potentially appearing specific to the case at hand, we believe that the current results hold significant weight in more general and complex learning problems as well. If we return to the case originally proposed in Sec. I, we recall that MultKAN there was suggested to learn xy as $[f_a(x) + g_a(y)] \cdot [f_m(x) + g_m(y)]$, finally converging to $f_a(x) = x, g_a(y) = 0, f_m(x) = 0$, and $g_m(y) = y$. The results of Fig. 2 appear to suggest that the presence of the “dummy” activations $g_a(y) = 0$ and $f_m(x) = 0$ impair the expressivity and training dynamics of MultKAN, lending it to slow convergence and counterintuitively nonzero $g_a(y)$ and $f_m(x)$ functions (i.e. nonzero grey starred activations in Fig. 1(A)) that add computational complexity and visual clutter impairing training and human-readability. In other words, MultKAN’s extraneous bulk means that it does not necessarily snap to the trivial solution even in a trivial training case, which may be of concern for users looking to model more complex phenomena that would likely exacerbate these issues. Its struggle (relative to LeanKAN) to learn the basic multiplication operator in a multidimensional case can be traced directly to specific terms and activations in its formulation, leading us to believe that this relative weakness compared to LeanKAN is not an artifact of a manufactured case, but rather an inherent performance drawback that may scale to other applications. While LeanKAN might not be guaranteed to perform in other applications as well as it did here, we can at least observe that it not only performed better via standard loss metrics, but also appeared to snap rapidly to the intuitive and interpretable result, properly zeroing out the unnecessary grey starred activations in Fig. 1(B).

3. Higher Order Multiplication

Such benefits become more significant when a higher order of multiplication is needed. For example, in the same problem setup, an additional output node $z_5 = x_1x_2x_3$ could be learned simply by selecting the structural hyperparameter $n^{mu} = 3$ in our LeanKAN, which does not change the number of activation functions or parameters. Interpretation-wise, we might expect to see three zero-offset identity functions in the fifth nodes for these three inputs. For MultKAN, however, k would need to increase to 3 to accommodate third-order multiplication, resulting in 16 additional activation functions compared to LeanKAN (and 2 times the total activation parameters). As a result, a single MultKAN layer risks blowing out the number of activation functions and dummy activations to learn higher order multiplication, worsening the memory efficiency and training efficiency while also concealing the interpretation of the true underlying behavior under a series of extraneous activations and operations. Partial mitigation of this issue is perhaps possible by optimizing the two hyperparameters, k and $1 - n^a$, for the order of multiplication and the number of output multiplication nodes, respectively. That being said, these two degrees of freedom add significant

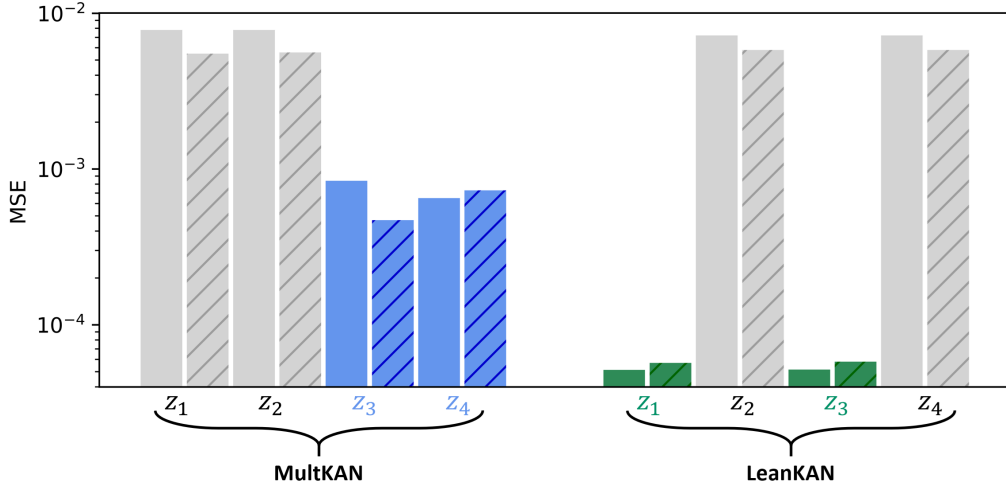


FIG. 3. Loss metrics after 3000 epochs. Solid bars are training, while striped bars are testing. Colored bars (blue and green for MultKAN and LeanKAN, respectively) indicate multiplication-enabled nodes, while grey bars are failed addition nodes. LeanKAN learns multiplication nodes with substantially higher accuracy while using fewer parameters.

complexity to the network designers' hyperparameter tuning task, and as discussed above $k = 3$ is already the most parameter-lean value possible for third-order multiplication. Conversely, LeanKAN has only one hyperparameter n^{mu} for the number of output multiplication nodes, with full utilization of all multiplication inputs (i.e. the order of multiplication is equal to the number of multiplication inputs), and with no changes to the parameter counts regardless of the value of n^{mu} .

For practical use, we suggest setting n^{mu} to half of the input size initially, for a balance between addition and multiplication nodes. Physical insights in the specific problem at hand may lead users to increase or decrease this value, at no parameter cost. Additionally, following from the discussion above, we suggest general use of LeanKAN in a two-layer structure: an input AddKAN layer to compose hidden node values that distribute all inputs across the entire width of the hidden layer, and then an output LeanKAN layer to inject sparse multiplication into the input-diverse hidden layer values. In doing so, users can completely negate the input-splitting issue seen in z_2 and z_4 in Figs. 2(B) and 2(D). In an extreme case where physical insights support the sole use of multiplication, a single-layer LeanKAN with $n^{mu} = n$ can also avoid this issue by applying multiplication to all nodes (similarly to how an AddKAN avoids this issue by applying addition to all nodes). By taking one of these two approaches, users can benefit from the substantial parameter savings of LeanKAN at a change in accuracy and training dynamics that, according to the results of Fig. 3, appears to be favorable to LeanKAN. In the next section, we learn simple biological dynamics via LeanKAN in an augmented architecture to investigate whether its lean parameterization can scale up to a more realistic case and continue to provide these counterintuitive performance improvements.

B. LeanKAN in Ordinary Differential Equations

In this section, we further investigate the quantitatively improved performance of LeanKAN compared to MultKAN in the respective optimal configurations: MultKAN is studied as the first of two layers (with the second being a standard additive KAN), and LeanKAN is studied as the second of two layers (the first similarly being a standard additive KAN). In doing so, all issues regarding input or output multiplication limitations (as studied in Fig. 2) are resolved.

In this case study, we look into the classical Lotka-Volterra predator-prey model using the Kolmogorov-Arnold Network Ordinary Differential Equation (KAN-ODE) framework of Koenig et al. [5]. Our aim here is to demonstrate LeanKAN as an effective layer structure in augmented KAN-based architectures (like KAN-ODEs). Briefly, and as was presented in more detail in Koenig et al. [5], the governing equations given the state variables $\mathbf{u} = [x, y]$ are

$$\begin{aligned} \frac{dx}{dt} &= \alpha x - \beta xy, \\ \frac{dy}{dt} &= \gamma xy - \delta y, \end{aligned} \tag{16}$$

with $\alpha = 1.5$, $\beta = 1$, $\gamma = 1$, and $\delta = 3$ and an initial condition of $\mathbf{u}_0 = [x_0, y_0] = [1, 1]$. The training data is generated in time span of $t \in [0, 3.5]$ s, while the unseen testing data is generated in the time span of $t \in [3.5, 14]$ s. The KAN-ODEs learn the underlying model as

$$\frac{d\mathbf{u}}{dt} = \text{KAN}(\mathbf{u}(t), \boldsymbol{\theta}), \quad (17)$$

where $\boldsymbol{\theta}$ is the collection of all trainable parameters in the KAN. Using the mean squared error (MSE) loss function and the adjoint sensitivity analysis [19, 20] as in Koenig et al. [5], we update $\boldsymbol{\theta}$ from a random initialization to fit the training data. The ADAM optimizer [18] was adopted with a learning rate of $2 \cdot 10^{-4}$ for both LeanKAN-based and MultKAN-based architectures in the fully converged cases of Secs. IV B 1 and IV B 2, and $5 \cdot 10^{-3}$ in the rapid convergence test of Sec. IV B 3.

1. Training Improvements with Large KANs

We first note the optimal KAN structure reported in Koenig et al. [5], which had a two-node input, a ten-node hidden layer, and a two-node output layer, all using standard AddKAN connections. All activations had five grid points each, and as in the first example here used RBF basis functions with a Swish basis residual function. This KAN contained 240 parameters. Here, we use it as the basis on which to design MultKAN and LeanKAN based networks.

As proposed in Sec. IV A, the LeanKAN model used here involves replacing the second layer of the original KAN structure of [5]. Instead of 20 additive KAN activations connecting the ten hidden nodes with the two output nodes, we choose $n^{mu} = 5$ to split the input nodes half and half between additive and multiplicative KAN operations. The overall structure remains as 2 nodes into 10 nodes into 2 nodes, for a conserved total of 240 parameters.

Separately, the MultKAN model used here involves replacing the first (input) layer of the original KAN structure of [5]. We similarly choose $n^a = 5$ to split the hidden nodes half and half between identity and multiplication operations. With the smallest multiplication order possible in the MultKAN framework, $k = 2$, the MultKAN parameter inflation leads to 300 total parameters, rather than 240 (half of the activations in the formerly 120-parameter MultKAN layer are doubled, for a total increase of 60 parameters). We also remark that $k = 2$, in a certain sense, contains inductive bias relevant to the problem at hand. Knowing that the governing equations in Eq. 16 contain second-order multiplication only, the MultKAN is encoded to contain only second-order multiplication structures. LeanKAN, on the other hand, has an order of multiplication equal to n^{mu} , and does not benefit from a problem-knowledge-enforced multiplication order. Both two-layer structures (as well as the original AddKAN structure of [5]) are visualized in Fig. 4(A).

Both models are trained for a relatively long 10^6 epochs, which in both cases takes on the order of tens of hours on a single CPU. Mean squared error results are compared across these network structures in Figs. 4(B-C) for training and testing losses, respectively. In the early epochs of training (up to and around $2 \cdot 10^5$ epochs), we see a remarkable improvement in training loss behavior from the MultKAN to the LeanKAN. Both converge fairly well to low loss, but the LeanKAN is rapidly able to reach a minimum value two orders of magnitude smaller than that of the MultKAN in these early epochs. In the testing loss results of Fig. 4(C), we see an even more pronounced discrepancy in the extremely early epochs, where the LeanKAN is almost immediately able to jump down to the 10^{-4} MSE range, while the MultKAN experiences a rather long delay while it finds its way below even just an MSE value of 1.

Looking out to the rest of the training window, we see that MultKAN is able to break into the 10^{-5} MSE range on training error after around $5 \cdot 10^5$ epochs, but is still never able to reach the sub- 10^{-6} value that the LeanKAN reaches in just $2 \cdot 10^5$ epochs. The testing losses, once the MultKAN is given enough time to converge, are fairly similar. It should be highlighted that the LeanKAN appears to have matched or outperformed the MultKAN with 60 fewer parameters (240 for LeanKAN and 300 for MultKAN).

To summarize, in this case with a relatively large KAN size and a long training window, we find that LeanKAN appears to outperform MultKAN in most aspects: it achieves a lower training loss, converges faster, and has a lower parameter count and complexity (even with the minimum $k = 2$ for the MultKAN). In the two following sections, we further probe these noteworthy performance improvements. First, to further elucidate the increased converged performance seen in the LeanKAN and test its robustness, we carry out a traditional neural convergence study to evaluate this behavior across networks of various node counts and grid densities. Then, to further study the improved early-epoch training dynamics seen in Figs. 4(B-C), we carry out a heavily restricted training cycle with smaller networks and just 7,000 epochs. We alternate in these two comparisons between identical network structures (with MultKAN benefitting from more parameters) and identical parameter counts (with MultKAN facing reduced nodes due to its extraneous activations) to further probe the parameter size discrepancy between architectures.

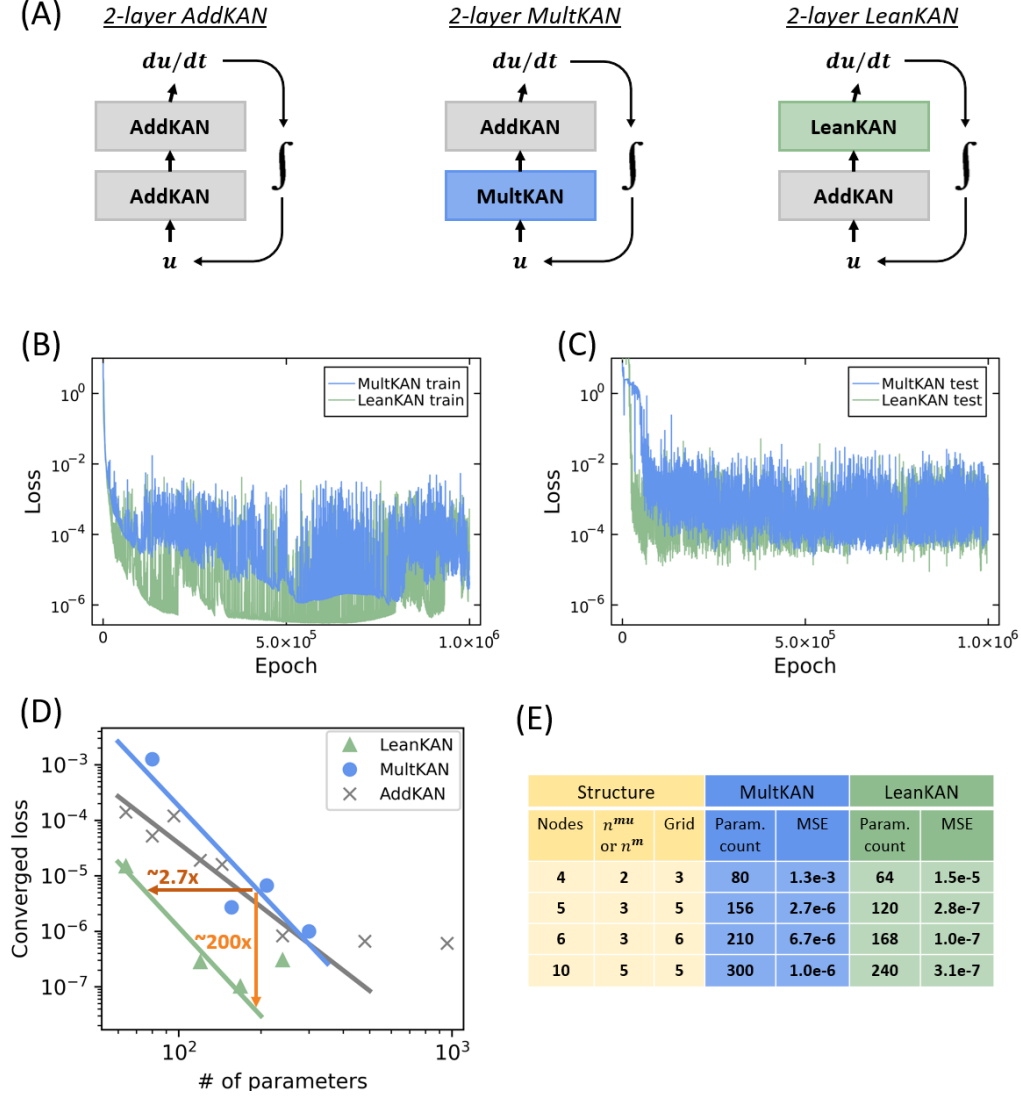


FIG. 4. Fully converged Lotka-Volterra inference comparisons between LeanKAN and MultKAN. (A) KAN-ODE layer structures referenced in the remaining subfigures. AddKAN is reported fully in [5]. (B-C) Training and testing results, respectively, with different traces representing the MultKAN and LeanKAN profiles. Both structures have a single hidden layer of 10 nodes, half of which are multiplication nodes, on a 5-point grid (300 MultKAN parameters and 240 LeanKAN parameters). (D-E) Neural convergence study comparing the two KAN layer architectures at various node and grid layouts, with the AddKAN convergence results of [5] plotted in grey. LeanKAN is seen to outperform MultKAN at all tested sizes, despite having 25% fewer parameters for a given size. Linear fit to convergence results suggest that while convergence rates are similar, LeanKAN has fewer extraneous parameters, shifting its linear fit significantly toward smaller parameter counts (see orange arrows for the average quantitative impact on the number of parameters and loss metrics). Linear fits for LeanKAN and AddKAN include only those points occurring before loss saturation.

2. Neural Convergence Comparison

We have identified in the results of Sec. IV A as well as Sec. IV B 1 that even with reduced parameter counts, LeanKAN appears to be able to slightly outperform MultKAN. We believe that this performance boost stems largely from the improved parameter efficiency of LeanKAN. While LeanKAN and MultKAN should both be able to converge to similar levels of loss when given arbitrarily many nodes and parameters, it is noteworthy that LeanKAN can do so with what appears to be significantly fewer parameters thanks to its elimination of dummy activations and extraneous parameters. To further test this behavior, we show neural convergence results for this example in Figs. 4(D-E). Testing across a range of identical node and grid structures of varying parameter counts, we see nearly identical neural scaling orders between MultKAN and LeanKAN (5.2 vs. 5.3, respectively). However, the entire curve for LeanKAN is shifted

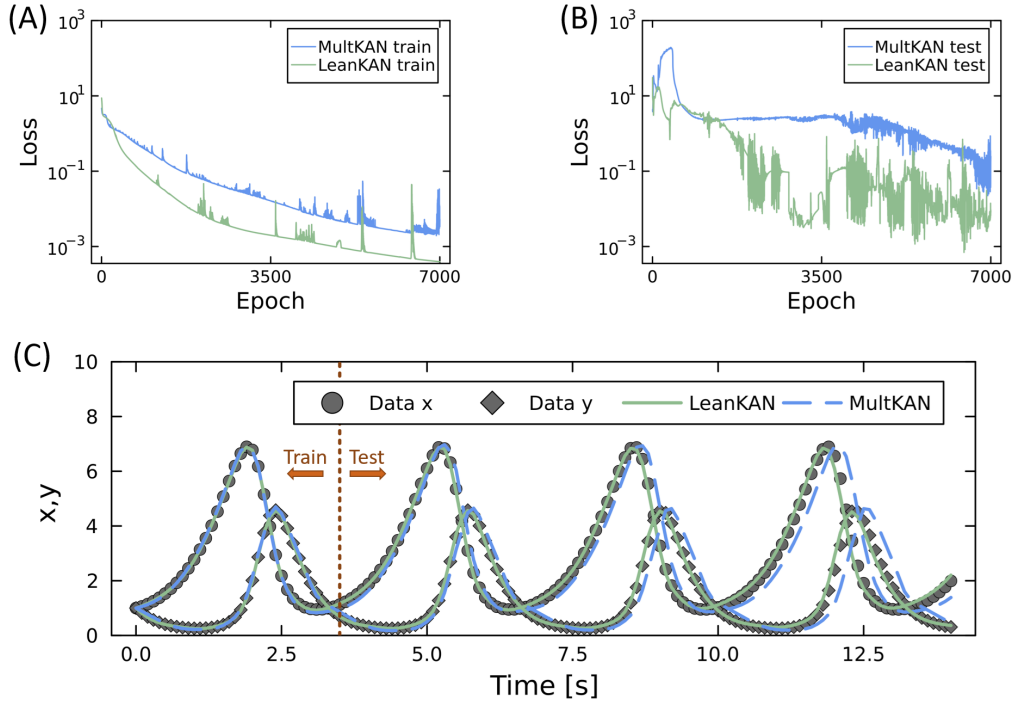


FIG. 5. Transient training dynamics comparison between LeanKAN and MultKAN for Lotka-Volterra system. (A-B) Training and testing results, respectively, with small KAN sizes (100 parameters) and 7000 epochs of training only. In addition to improved converged results (Fig. 4), LeanKAN is seen to have further improved transient training dynamics. (C) Training and testing data reconstruction using the results of (A-B). Both KAN architectures appear to predict the training data sufficiently well, though MultKAN struggles more with the unseen testing data.

significantly to the left, indicating that while both are capable of achieving the same neural scaling and final strong performance, LeanKAN is simply able to do so with fewer parameters. In fact, the LeanKAN was able to converge to its minimum loss value (where larger networks provide no additional accuracy) with just 168 parameters, while the MultKAN appears to be not yet fully converged even with 300 parameters. Specifically, for a given MultKAN parameter count and converged loss, LeanKAN is capable of achieving the same converged loss with 2.7 times fewer parameters on average. Alternatively, the LeanKAN with the same number of parameters is capable of achieving 200 times less converged loss on average.

In Fig. 4(D) we additionally plot the neural convergence behavior of AddKAN layers reported in [5], with identical other hyperparameters, Lotka-Volterra coefficients, training windows, etc. Based on discussion in [1, 2], we would expect any multiplication-based KAN layer to benefit in this case, which as per Eq. 16 depends heavily on multiplication. A KAN based solely on addition is forced to carry out bulky and parameter-inefficient operations such as $xy = ((x + y)^2 - (x^2 + y^2))/2$ in order to represent the Lotka-Volterra dynamics, while multiplication-based layers can directly represent xy . It appears, however, that while MultKAN may benefit from this efficient multiplication representation, any such benefits are negated by the extraneous parameters contained in its dummy activations. The end result is stagnant neural convergence behavior (roughly the same rate and same location as in the AddKAN networks). LeanKAN, on the other hand, is able to exploit this lean multiplication representation without the drawback of extraneous parameters or dummy activations, allowing it to shift its entire curve to substantially lower losses and parameter counts.

3. Increased Convergence Speed

The last behavior that we noted in Figs. 4(B-C) is the improved transient training dynamics of LeanKAN. To further test this behavior, we replace the large-model, long-window training used in Figs. 4(B-C) with smaller models and shorter training times that are more indicative of potential real-world application (especially in a case with simple 1-D trajectories like is studied here).

In all previous cases, we used identical node structures in MultKAN and LeanKAN, which inherently leads to larger MultKAN parameter counts. Here, we instead equalize the number of parameters in both networks. The

MultKAN structure is reduced to four hidden nodes (with $n^a=2$ for two multiplication and two addition nodes) and four gridpoints, with 100 total parameters. The LeanKAN structure, meanwhile, is reduced to five hidden nodes (with $n^{mu} = 3$ for three multiplication and two addition nodes) with the same four gridpoints, resulting in 100 total parameters. This reduction of LeanKAN to the same parameter count with an additional hidden node compared to MultKAN is possible thanks to its compact form compared to even the smallest ($k = 2$) MultKAN, and its ability to represent multiplication nodes using fewer parameters and fewer activations.

Both networks in this case are trained for relatively small 7,000 epochs (chosen to allow the MultKAN enough training time to fit the testing data passably well). Training dynamics are shown in Figs. 5(A-B). Looking first at the training loss and training data reconstruction, we notice that the LeanKAN training loss rapidly drops below that of the MultKAN and is nearly an order of magnitude less than that of the MultKAN for the entire training window. This corroborates the behavior seen at early epochs in Fig. 4(B). In the data reconstruction of Fig. 5(C), both fit the training data strongly on inspection, although a very close look shows that the MultKAN, especially toward the end of the 3.5 s training window, begins to diverge from the data.

Looking next at the testing data, we see further corroboration of the distinction originally noted in Fig. 4(C). That is, the LeanKAN is rapidly able to capture the behavior of the underlying model and drop its testing loss to acceptably low values, while the MultKAN struggles and does not begin to notably decrease its testing loss until after 5,000 epochs have passed. In the testing window reconstruction of Fig. 5(C), this distinction is obvious. The LeanKAN fits the unseen data very well and does not begin to deviate notably until the last oscillation, while the MultKAN almost immediately diverges from the testing data and has significant error by the final oscillation.

To summarize, the three tests carried out using the Lotka-Volterra equations in the KAN-ODE framework found that LeanKAN appears to outperform MultKAN in most metrics across the board. Both are able to achieve strong accuracy in most cases, but LeanKAN is able to converge faster, to lower loss values, and with significantly fewer parameters than MultKAN. Some of the bulk in MultKAN that leads to these performance drawbacks is likely able to be pruned downstream, as studied in [1, 2, 5], although in the cases studied here we saw no reason to begin optimization at such a heavily parameterized structure in the first place, as the leaner and still-prunable LeanKAN saw superior performance across all metrics.

V. CONCLUSIONS

In this work we proposed LeanKAN as an alternative to MultKAN for incorporating multiplication nodes into KAN layers. While MultKAN is not suitable for general use in a multidimensional output layer, LeanKAN’s reversed structure lends it to global use in output layers (at the cost of its lack of use for input layers). LeanKAN is also parameterized more compactly than MultKAN and is inherently less complex with fewer activations and fewer parameters for a given number of layers, nodes, and gridpoints. In a similar vein, it eliminates one of two multiplication hyperparameters, simplifying the network tuning process.

LeanKAN is a one-to-one replacement for standard AddKAN or MultKAN layers, lending it to use not just in standard KAN applications, but also in augmented network structures based on KAN. In the two case studies presented here, we demonstrate LeanKAN’s performance both as a standard KAN layer in a toy multiplication reconstruction case, and also as the backbone of a KAN-ODE. Across the board, we found that LeanKAN’s compact structure did not carry any performance downgrades. In fact, LeanKAN was found to significantly outperform similarly sized and even substantially larger MultKANs in all studied metrics, thanks to its elimination of dummy activations and extraneous parameters. For general use in KANs with multiplication-based layers, we hope these results inspire adoption of LeanKANs as a simpler, leaner, and faster layer structure.

DATA AND MATERIALS AVAILABILITY

The LeanKAN code will be made public upon acceptance of the manuscript.

ACKNOWLEDGEMENT

This work is supported by the National Science Foundation (NSF) under Grant No. CBET-2143625. BCK is partially supported by the NSF Graduate Research Fellowship under Grant No. 1745302.

CREDIT AUTHORSHIP CONTRIBUTION STATEMENT

Benjamin C. Koenig: Conceptualization, Methodology, Software, Investigation, Writing - Original Draft. **Suyong Kim:** Conceptualization, Methodology, Writing - Original Draft, Writing - Review & Editing. **Sili Deng:** Funding Acquisition, Resources, Writing - Review & Editing.

DECLARATION OF COMPETING INTEREST

The authors declare that they have no known competing financial interests or personal relationships that could have appeared to influence the work reported in this paper.

-
- [1] Z. Liu, Y. Wang, S. Vaidya, F. Ruehle, J. Halverson, M. Soljačić, T. Y. Hou, M. Tegmark, KAN: Kolmogorov-Arnold Networks (2024). doi:10.48550/arXiv.2404.19756.
 - [2] Z. Liu, P. Ma, Y. Wang, W. Matusik, M. Tegmark, KAN 2.0: Kolmogorov-Arnold Networks Meet Science (2024). doi:10.48550/arXiv.2408.10205.
 - [3] A. N. Kolmogorov, On the representation of continuous functions of several variables as superpositions of continuous functions of a smaller number of variables., Dokl. Akad. Nauk (108(2)) (1956).
 - [4] A. Ismayilova, V. E. Ismailov, On the Kolmogorov neural networks, Neural Networks 176 (2024) 106333. doi:10.1016/j.neunet.2024.106333.
 - [5] B. C. Koenig, S. Kim, S. Deng, KAN-ODEs: Kolmogorov-Arnold network ordinary differential equations for learning dynamical systems and hidden physics, Computer Methods in Applied Mechanics and Engineering 432 (2024) 117397. doi:10.1016/j.cma.2024.117397.
 - [6] S. Patra, S. Panda, B. K. Parida, M. Arya, K. Jacobs, D. I. Bondar, A. Sen, Physics Informed Kolmogorov-Arnold Neural Networks for Dynamical Analysis via Efficient-KAN and WAV-KAN (2024). doi:10.48550/arXiv.2407.18373.
 - [7] C. Guo, L. Sun, S. Li, Z. Yuan, C. Wang, Physics-informed Kolmogorov-Arnold Network with Chebyshev Polynomials for Fluid Mechanics (2024). doi:10.48550/arXiv.2411.04516.
 - [8] A. A. Howard, B. Jacob, S. H. Murphy, A. Heinlein, P. Stinis, Finite basis Kolmogorov-Arnold networks: domain decomposition for data-driven and physics-informed problems (2024). doi:10.48550/arXiv.2406.19662.
 - [9] A. D. Bodner, A. S. Tepsich, J. N. Spolski, S. Pourteau, Convolutional Kolmogorov-Arnold Networks (2024). doi:10.48550/arXiv.2406.13155.
 - [10] D. W. Abueidda, P. Pantidis, M. E. Mobasher, DeepOKAN: Deep operator network based on Kolmogorov Arnold networks for mechanics problems, Computer Methods in Applied Mechanics and Engineering 436 (2025) 117699. doi:10.1016/j.cma.2024.117699.
 - [11] A. Kashefi, Kolmogorov-Arnold PointNet: Deep learning for prediction of fluid fields on irregular geometries (2024). doi:10.48550/arXiv.2408.02950.
 - [12] K. Hornik, M. Stinchcombe, H. White, Multilayer feedforward networks are universal approximators, Neural Networks 2 (5) (1989) 359–366. doi:10.1016/0893-6080(89)90020-8.
 - [13] Z. Li, Kolmogorov-Arnold Networks are Radial Basis Function Networks (2024). doi:10.48550/arXiv.2405.06721.
 - [14] Blealtan, efficient-kan, GitHub repository. Retrieved from <https://github.com/Blealtan/efficient-kan> (2024).
 - [15] V. Puri, KolmogorovArnold.jl, GitHub repository. Retrieved from <https://github.com/vpuri3/KolmogorovArnold.jl> (2024).
 - [16] P. Ramachandran, B. Zoph, Q. V. Le, Searching for Activation Functions (2017). doi:10.48550/arXiv.1710.05941.
 - [17] Y. Wang, J. Sun, J. Bai, C. Anitescu, M. S. Eshaghi, X. Zhuang, T. Rabczuk, Y. Liu, Kolmogorov Arnold Informed neural network: A physics-informed deep learning framework for solving forward and inverse problems based on Kolmogorov Arnold Networks, Computer Methods in Applied Mechanics and Engineering 433 (2025) 117518. doi:10.1016/j.cma.2024.117518.
 - [18] D. P. Kingma, J. Ba, Adam: A Method for Stochastic Optimization (2017). doi:10.48550/arXiv.1412.6980.
 - [19] R. T. Q. Chen, Y. Rubanova, J. Bettencourt, D. Duvenaud, Neural Ordinary Differential Equations (2019). doi:10.48550/arXiv.1806.07366.
 - [20] C. Rackauckas, Y. Ma, J. Martensen, C. Warner, K. Zubov, R. Supekar, D. Skinner, A. Ramadhan, A. Edelman, Universal Differential Equations for Scientific Machine Learning (2021). doi:10.48550/arXiv.2001.04385.